Density, Viscosity and Free Energy of Activation for Viscous Flow of Monoethanol Amine (1) + H$_2$O (2) + CO$_2$ (3) Mixtures

Sumudu S. Karunarathne [ID] **, Dag A. Eimer and Lars E. Øi ***

Faculty of Technology, Natural Sciences and Maritime Studies, University of South-Eastern Norway, Kjølnes Ring 56, 3901 Porsgrunn, Norway; sumuduunimrt@gmail.com (S.S.K.); dag.a.eimer@usn.no (D.A.E.)
* Correspondence: lars.oi@usn.no; Tel.: +47-35575141

Abstract: Densities and viscosities of aqueous monoethanol amine (MEA) and CO$_2$-loaded aqueous MEA are highly relevant in engineering calculations to perform process design and simulations. Density and viscosity of the aqueous MEA were measured in the temperature range of 293.15 K to 363.15 K with MEA mass fractions ranging from 0.3 to 1.0. Densities of the aqueous MEA were fitted for a density correlation. Eyring's viscosity model based on absolute rate theory was adopted to determine the excess free energy of activation for viscous flow of aqueous MEA mixtures and was correlated by a Redlich–Kister polynomial. Densities and viscosities of CO$_2$-loaded MEA solutions were measured in the temperature range of 293.15 K to 353.15 K with MEA mass fractions of 0.3, 0.4 and 0.5. The density correlation used to correlate aqueous MEA was modified to fit CO$_2$-loaded density data. The free energy of activation for viscous flow for CO$_2$-loaded aqueous MEA solutions was determined by Eyring's viscosity model and a correlation was proposed to represent free energy of activation for viscous flow and viscosity. This can be used to evaluate quantitative and qualitative properties in the MEA + H$_2$O + CO$_2$ mixture.

Keywords: density; viscosity; Eyring's viscosity model; MEA

1. Introduction

Post-combustion CO$_2$ capture (PCC) using absorption and desorption has gained great attention in the last decades and several amines have been investigated for their absorption efficiency. In acid gas treatment, monoethanol amine (MEA, IUPAC name: 2-aminoethanol) has been used since 1930 [1]. It is the benchmark amine for the evaluation of other amines in CO$_2$ capture performance considering absorption efficiency, reaction rates, energy demand and corrosion resistance. A blend of 30% MEA with 70% H$_2$O by mass is a standard in PCC. Higher reaction rates of MEA with CO$_2$ compared to secondary and tertiary amines enables optimization of the dimensions and operational parameters of the absorber column. MEA's low-absorption capacity and high-energy demand for desorption and poor corrosion resistance are arguments against the use of MEA at the commercial scale [2,3].

Density and viscosity of pure, aqueous and CO$_2$-loaded aqueous MEA have been studied and reported in the literature under different temperatures, MEA concentrations and CO$_2$ loadings [1,4–12]. These data are vital for development of empirical correlations that are useful in various aspects of process equipment design and process simulations. Density is important to determine the physical solubility of CO$_2$ in solvent, the solvent kinetics and mass transfer. Viscosity is frequently used in the modified Stoke–Einstein equation to estimate diffusivity that is necessary for calculating mass transfer and kinetic properties [13,14]. Many references are available for data of aqueous MEA solutions under different MEA concentrations and temperatures. There is a lack of measured data for physical properties

of CO_2-loaded solutions at different CO_2 loadings under different MEA concentrations. In order to reduce the unmeasured regions and to check the validity of measured data, further experimental studies are necessary.

Amundsen, Øi and Eimer [6] have used the McAllister three-body model [15] to represent the kinematic viscosity. Weiland, Dingman, Cronin and Browning [9] and Hartono, Mba and Svendsen [10] measured both density and viscosity of CO_2-loaded aqueous MEA solutions and proposed correlations to fit the data. The approach of using a Redlich-Kister [16] type polynomial to predict excess volume for the aqueous MEA solutions in the density correlations is widely used. A similar approach to correlate excess viscosity is adopted by Islam, et al. [17] for aqueous MEA.

In this work, density and viscosity of aqueous MEA and CO_2-loaded aqueous MEA were measured. The density correlation proposed by Aronu, Hartono and Svendsen [14] for the aqueous amino acid salt and amine amino acid salt solutions was used to correlate the density data of aqueous MEA. The same correlation was modified to predict the density of CO_2-loaded aqueous MEA solutions. The parameters of the correlations were found through a regression analysis. Eyring's viscosity model [18] was used to calculate the free energy of activation for viscous flow of the aqueous MEA solutions and parameters of the Redlich-Kister type polynomial were estimated by regression. For the viscosity of CO_2-loaded solutions, the difference of activation energy between CO_2-loaded aqueous MEA and aqueous MEA solutions were calculated, and a correlation was proposed.

2. Materials and Methods

2.1. Sample Preparation and CO_2 Loading Analysis

Descriptions of materials used in this study are given in Table 1. The Milli-Q water (resistivity 18.2 MΩ·cm) was degassed using a rotary evaporator connected to a vacuum pump to remove any dissolved gasses. The weights of liquids were measured through an electronic balance from Mettler Toledo (XS403S, Mettler Toledo, Greifensee, Switzerland) with a resolution of 1 mg. Aqueous MEA solutions with MEA to H_2O mass ratio w_1 = 0.3, 0.4, and 0.5 were prepared and fully loaded by bubbling CO_2 through the solution until the pH become steady over time. Then different CO_2-loaded solutions were prepared by diluting them with corresponding aqueous MEA. The amount of CO_2 loaded to the aqueous MEA was determined by a titration method in which CO_2 was fixed as $BaCO_3$ via adding 50 mL of each 0.1 M NaOH and 0.3 M $BaCl_2$ to 0.1–0.2 g of CO_2 loaded solution. All the samples were boiled for approximately 10 min to ensure the completion of chemical reactions and were cooled until the temperature reaches the room conditions. Eventually, $BaCO_3$ was separated by filtering using a hydrophilic polypropylene membrane filter (47 mm, 0.45 μm). The filtered $BaCO_3$ was put into 100 mL of distilled water and titrated with 0.1 M HCl until the solution reached pH of 2. Meanwhile, care needed to be taken to make sure all the $BaCO_3$ was dissolved during the titration. Then, the sample was boiled and cooled again before it was titrated with 0.1 M NaOH. Finally, the MEA concentration of mixtures was determined by titrating 1 g of CO_2-loaded solution with 1 M HCl.

Table 1. Materials used in this study [a,b].

Chemical Name	CAS Reg. No.	Mole Fraction Purity [a]	Source	Purification
monoethanol amine (MEA)	141-43-5	≥0.995 (GC [b])	Sigma–Aldrich	no
carbon dioxide (CO_2)	124-38-9	0.99999	AGA Norge AS	no
nitrogen (N_2)	7727-37-9	0.99999	AGA Norge AS	no
sodium hydroxide (NaOH)	1310-73-2	-	Merck KGaA	no
hydrochloric acid (HCl)	7647-01-0	-	Merck KGaA	no
barium chloride dihydrate ($BaCl_2 \cdot 2H_2O$)	10326-27-9	≥0.99	Merck KGaA	no

[a] As mentioned by the supplier. [b] Gas-liquid chromatography.

2.2. Density Measurements

The density of aqueous MEA and CO_2-loaded aqueous MEA was measured by a DMA 4500 density meter from Anton Paar (Graz, Austria). The standard calibration procedure for DMA 4500 was performed using degassed water and air at 293.15 K occasionally, while density checks were performed frequently to check the validity of the previous calibration at 293.15 K. Samples were inserted into the U-tube with care to prevent the presence of air bubbles in the tube. Measurements were performed using a separate sample at each temperature and composition. A cleaning and drying process of the U-tube was performed every time before a new sample was introduced. Density measurements were performed for the aqueous MEA of w_1 from 0.3 to 1 for the temperature range from 293.15 K to 363.15 K and CO_2-loaded aqueous MEA of w_1 = 0.3, 0.4 and 0.5 under different CO_2 loading for the temperature range from 293.15 K to 353.15 K. Final density data are presented as an average of three density measurements at each temperature and composition.

2.3. Viscosity Measurements

The dynamic viscosity was measured using a double-gap concentric rheometer Physica MCR 101 from Anton Paar (pressure cell XL DG35.12/PR; measuring cell serial number 80462200) (Graz, Austria). The standard viscosity solution S3S from Paragon Scientific Ltd. was used to calibrate the rheometer at different temperatures. The calibration and the measurement were done by using 7 mL of liquid volume under the shear rate (γ) of 1000 s^{-1}. Having compared with the reference viscosity data, measured viscosities of standard viscosity solution were used to determine the viscosity deviations at different temperatures. For temperatures where the supplier did not specify any reference viscosities, expected viscosity deviations were obtained via interpolation. A temperature controlling system with standard temperature uncertainty of ±0.03 K is equipped with the rheometer. An external cooling system of Anton Paar Viscotherm VT2 (Graz, Austria) with standard temperature uncertainty of ±0.02 K is employed for better temperature control in the range from 293.15 K to 303.15 K. The solution in the rheometer was pressured by N_2 gas (p = 4 bar) to minimize the possible release of MEA and CO_2 into the gas phase. Viscosity measurements were performed for the aqueous MEA of w_1 from 0.3 to 1 in the temperature range from 293.15–363.15 K and CO_2-loaded aqueous MEA with w_1 = 0.3, 0.4 and 0.5 under different CO_2 loadings for the temperature range from 293.15 K to 353.15 K. The viscosity data presented in this study are the averaged measurements for minimum of three different measurements.

3. Experimental Uncertainty

The Guide to the expression of Uncertainty in Measurement (GUM) [19,20] approach was adopted for the uncertainty evaluations using the mathematical models defined for the instruments for density and viscosity measurements. Several uncertainty sources including purity of MEA, weight measurements, repeatability, CO_2 loading and temperature were considered in addition to the uncertainty sources in the model equations during the uncertainty evaluation. The temperature accuracy of DMA 4500 and Physica MCR 101 Anton Paar are both specified as ±0.03 K. Considered standard uncertainties u for the density measurements are $u(\alpha)$ = ±0.005 (CO_2 loading mol CO_2/mol MEA), $u(w)$ = ±2 × 10^{-4} kg (weight measurement), $u(p)$ = ±0.003 (MEA purity), $u(T)$ = ±0.012 K (temperature) and $u(rep)$ = ±0.13 kg·m^{-3} (repeatability). The gradient $\partial\rho/\partial T$ of density against temperature was found as 0.73 kg·m^{-3}·K^{-1} and the corresponding uncertainty in ρ that is $(\partial\rho/\partial T)\,u(T)$ was calculated as ±0.009 kg·m^{-3}. The gradient of density against CO_2 loading, $\partial\rho/\partial\alpha$, was found as 334 kg m^{-3} and the corresponding uncertainty in ρ, $(\partial\rho/\partial\alpha)\,u(\alpha)$ was found as ±1.67 kg·m^{-3}. The standard combined uncertainty for density measurement $u(\rho)$ was found as $u(\rho)$ = ±3.90 kg·m^{-3}. Accordingly the combined expanded uncertainty $U_c(\rho)$ for density of CO_2-loaded aqueous MEA is $U_c(\rho)$ = ±7.80 kg·m^{-3} (level of confidence = 0.95, where k = 2).

The considered standard uncertainties u for the viscosity measurements are $u(\alpha)$ = ±0.005 (CO_2 loading mol CO_2/mol MEA), $u(w)$ = ±2 × 10^{-4} kg (weight measurement), $u(p)$ = ±0.003 (MEA purity),

$u(T) = \pm0.012$ K (temperature) and $u(rep) = \pm0.008$ mPa·s (repeatability). The standard combined uncertainty for viscosity measurement $u(\eta)$ was found as $u(\eta) = \pm0.018$ mPa·s. Accordingly the combined expanded uncertainty U_c is $U_c(\eta) = \pm0.036$ mPa·s (level of confidence = 0.95, where $k = 2$).

4. Results and Discussion

This section discusses the density, viscosity and free energy of activation for viscous flow in aqueous and CO_2-loaded aqueous MEA solutions. The correlations to represent density and viscosity data were evaluated using average absolute relative deviation and absolute maximum deviation (AARD and AMD) as given in Equations (1) and (2).

$$AARD(\%) = \frac{100\%}{N} \sum_{i=1}^{N} \left| \frac{Y_i^E - Y_i^C}{Y_i^E} \right| \tag{1}$$

$$AMD = MAX \left| Y_i^E - Y_i^C \right| \tag{2}$$

where N, Y_i^E and Y_i^C refer the number of data points, the measured property and calculated property respectively.

4.1. Density of MEA (1) + H_2O (2) + CO_2 (3) Mixtures

Many approaches in density correlations are based on suggesting a Redlich–Kister polynomial to fit the excess volume properties of the mixture. One of the drawbacks of the excess volume approach using a Redlich–Kister polynomial to calculate density is the complexity of the correlation due to a high number of parameters. The density correlation proposed by Aronu, Hartono and Svendsen [14] as given by Equation (3) was used to fit the measured aqueous density data. The estimated parameters are presented in Table 2. The correlation was in good agreement with measured data with AARD = 0.12% for the w_1 range from 0.3 to 0.9. The same parameters were used to fit the density of CO_2-loaded solutions by introducing a function with new parameters for the temperature and CO_2 mole fraction as illustrated in Equation (4).

Table 2. Correlation parameters for density of aqueous MEA.

MEA/w_1	T/K	No. Points	Parameters
0.3–0.9	293.15–363.15	56	$k_1 = 683.5$ $k_2 = 1.344 \times 10^5$ $k_3 = -1.089 \times 10^4$ $k_4 = 145.2$ $k_5 = 567.9$
AARD (%)			0.12
AMD (kg·m^{-3})			3.45

Correlation for the density of aqueous MEA:

$$\rho = \left(k_1 + \frac{k_2 x_2}{T} \right) exp\left(\frac{k_3}{T^2} + \frac{k_4 x_1}{T} + k_5 \left(\frac{x_1}{T} \right)^2 \right) \tag{3}$$

where ρ, T, x_1, x_2 and k_i are density, temperature, mole fractions of MEA, H_2O of the aqueous mixture and estimated parameter vector.

The measured densities of aqueous MEA solutions are listed in Table 3. A comparison between correlations that are based on excess volume presented by Hartono, Mba and Svendsen [10] and Han, Jin, Eimer and Melaaen [1] with this work is shown in Figure 1. The accuracy of the correlation fit is acceptable compared to the literature [1,10]. The correlation deviates from measured density

with AMD of 3.45 kg·m^{-3} at $w_1 = 0.8$ and $T = 293.15$ K. This deviation is less than the measurement uncertainty reported in this study for aqueous MEA.

Table 3. Measured density ρ/kg·m^{-3} of aqueous MEA [a,b,c,d,e].

w_1	x_1	Measured Density ρ/kg·m^{-3}							
		293.15 K	**303.15 K**	**313.15 K**	**323.15 K**	**333.15 K**	**343.15 K**	**353.15 K**	**363.15 K**
0.3	0.1122	1012.6 1012.68 [d]	1008.2 1008.4 [b] 1008.31 [d] 1008.2 [e]	1003.3 1003.3 [b] 1003.4 [c] 1003.45 [d] 1003.3 [e]	997.9 998.1 [b] 998.1 [c] 998.07 [d] 998.1 [e]	991.6 992.3 [b] 992.23 [d] 992.3 [e]	986.0 986.1 [b] 985.8 [c] 985.96 [d]	979.4 979.4 [b] 979.4 [c] 979.27 [d]	972.3 972.5 [b]
0.4	0.1643	1018.4	1013.3 1013.8 [b] 1013.3 [e]	1007.8 1008.3 [b] 1007.7 [c] 1007.8 [e]	1001.8 1002.3 [b] 1001.8 [c] 1002.1 [e]	995.5 996.1 [b] 995.7 [e]	988.9 989.4 [b] 988.9 [c]	981.9 982.4 [b] 981.9 [c]	974.6 975.0 [b]
0.5	0.2278	1023.6	1017.8 1018.2 [b] 1017.8 [e]	1011.6 1012.1 [b] 1011.7 [c] 1011.8 [e]	1005.2 1005.6 [b] 1005.3 [c] 1005.4 [e]	998.4 999.0 [b] 998.7 [e]	991.4 991.9 [b] 991.5 [c]	984.1 984.5 [b] 984.2 [c]	976.4 976.9 [b]
0.6	0.3067	1027.7	1021.2 1021.4 [b] 1021.3 [e]	1014.5 1014.7 [b] 1014.6 [e]	1007.6 1007.8 [b] 1007.8 [e]	1000.4 1000.7 [b] 1000.6 [e]	993.0 993.2 [b]	985.4 985.6 [b]	977.4 977.7 [b]
0.7	0.4077	1029.3	1022.4 1022.8 [b] 1022.6 [e]	1015.2 1015.7 [b] 1015.5 [c] 1015.5 [e]	1007.9 1008.3 [b] 1008.2 [c] 1008.2 [e]	1000.4 1000.8 [b] 1000.6 [e]	992.7 993.1 [b] 993.0 [c]	984.8 985.2 [b] 985.0 [c]	976.4 977.1 [b]
0.8	0.5412	1028.1	1020.8 1021.0 [b]	1013.3 1013.5 [b]	1005.7 1005.9 [b]	997.9 998.2 [b]	990.0 990.2 [b]	981.9 982.1 [b]	973.6 973.9 [b]
0.9	0.7264	1023.5	1015.8 1016.2 [b]	1008.1 1008.5 [b] 1008.4 [c]	1000.3 1000.6 [b] 1000.6 [c]	992.4 992.7 [b]	984.3 984.6 [b] 984.6 [c]	976.1 976.5 [b] 976.4 [c]	967.8 968.1 [b]
1	1.0000	1015.9	1008.1 1008.0 [b]	1000.1 1000.0 [b] 1000.3 [c]	992.1 992.0 [b] 992.3 [c]	984.0 983.9 [b]	975.9 975.8 [b] 976.0 [c]	967.6 967.5 [b] 967.8 [c]	959.3 959.2 [b]

[a] Standard uncertainties u are $u(w) = \pm 2 \times 10^{-4}$ kg, $u(p) = \pm 0.003$, $u(T) = \pm 0.012$ K, $u(rep) = \pm 0.13$ kg·m^{-3}. The combined expanded uncertainty U_c is $U_c(\rho) = \pm 7.10$ kg·m^{-3} (level of confidence = 0.95, where $k = 2$). [b] Han, Jin, Eimer and Melaaen [1], [c] Amundsen, Øi and Eimer [6], [d] Hartono, Mba and Svendsen [10], [e] Jayarathna, Weerasooriya, Dayarathna, Eimer and Melaaen [8].
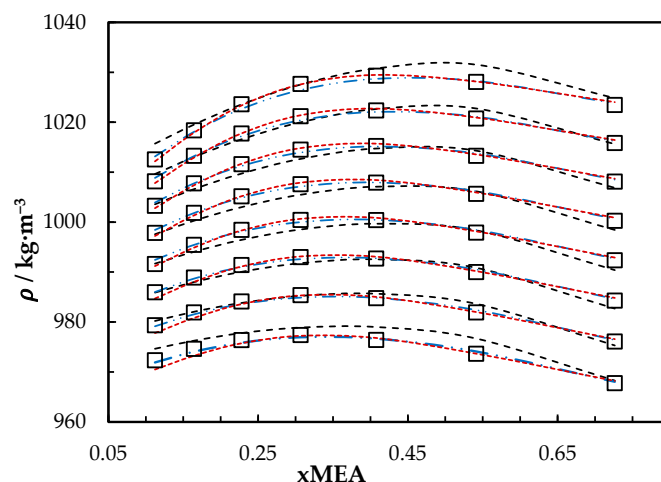
Figure 1. Density of aqueous MEA mixtures at different concentrations and temperatures (293.15, 303.15, 313.15, 323.15, 333.15, 343.15, 353.15 and 363.15) K. Data: from this work, '□'. Correlation predictions: from this work, '- - -'; Hartono, Mba and Svendsen [10], '----'; Han, Jin, Eimer and Melaaen [1], '· · ·'.

Correlation for the density of CO_2-loaded aqueous MEA:

$$\rho = (a_1 + a_2(T) + a_3(T)^2 + a_4 x_3)\left(k_1 + \frac{k_2 x_2}{T}\right)exp\left(\frac{k_3}{T^2} + \frac{k_4 x_1}{T} + k_5\left(\frac{x_1}{T}\right)^2\right) \tag{4}$$

The measured density of CO_2-loaded aqueous MEA of w_1 = 0.3, 0.4 and 0.5 solutions are shown in Table 4 and the correlation described in Equation (4) used to fit the data. At higher CO_2 loadings (α > 0.5), formation of air bubbles was noticed in the U-tube beyond temperatures of 323.15 K in DMA 4500. This increases the uncertainty of the density measurements. Accordingly, densities at temperatures up to 323.15 K are shown for the solutions with w_1 = 0.3 and 0.4. The same was observed for the solution of w_1 = 0.5 with α = 0.495 at above T = 343.15 K. Figure 2 shows the comparison of correlations proposed by Hartono, Mba and Svendsen [10], Han, Jin, Eimer and Melaaen [1] with this work for MEA solution of w_1 = 0.3. Measured densities at w_1 = 0.4 and 0.5 are given in Figures 3 and 4 with data from the literature. The correlation by Hartono, Mba and Svendsen [10] deviates positively from the measured data with AMD of 8.9 kg·m^{-3} while Han, Jin, Eimer and Melaaen [1] deviates negatively with AMD of 9.5 kg·m^{-3} at higher CO_2 loadings. The required parameters of Equation (4) for the CO_2-loaded solutions are listed in Table 5. The AMD from Equation (4) is lower than that from the other correlations.

Table 4. Measured density ρ/kg·m^{-3} of CO_2-loaded (α/mol CO_2·mol MEA^{-1}) aqueous MEA [a].

x_3	α	Measured Density ρ/kg·m^{-3}						
		293.15 K	303.15 K	313.15 K	323.15 K	333.15 K	343.15 K	353.15 K
w_1 = 0.3								
0.0000	0.000	1012.6	1008.2	1003.3	997.9	991.6	986.0	979.4
0.0105	0.095	1032.0	1027.6	1022.8	1017.4	1011.6	1005.1	995.5
0.0193	0.175	1052.5	1048.1	1043.3	1038.1	1032.4	1026.4	1020.1
0.0355	0.328	1077.8	1073.4	1068.6	1063.4	1057.9	1052.0	1044.1
0.0476	0.445	1103.3	1097.7	1092.8	1087.6	1082.1	1075.7	1069.3
0.0574	0.543	1123.1	1118.4	1113.4	1107.9			
w_1 = 0.4								
0.0000	0.000	1018.4	1013.3	1007.8	1001.9	995.5	988.9	981.9
0.0170	0.105	1045.6	1040.7	1035.3	1029.6	1023.6	1017.3	1010.6
0.0341	0.215	1073.4	1068.5	1063.3	1057.8	1051.9	1045.8	1039.4
0.0507	0.325	1102.0	1097.2	1092.0	1086.5	1080.8	1074.9	1068.6
0.0669	0.436	1130.3	1125.4	1120.2	1114.7	1109.2	1103.2	1097.0
0.0826	0.548	1155.5	1150.4	1145.1	1139.5			
w_1 = 0.5								
0.0000	0.000	1023.6	1017.8	1011.6	1005.2	998.4	991.4	984.1
0.0205	0.092	1052.3	1046.7	1040.9	1034.7	1028.3	1021.7	1014.8
0.0406	0.186	1082.4	1077.0	1071.4	1065.5	1059.4	1053.0	1046.4
0.0620	0.290	1112.7	1107.4	1101.9	1096.2	1090.3	1084.2	1077.9
0.0825	0.395	1144.5	1139.2	1133.8	1128.3	1122.5	1116.6	1110.5
0.1013	0.495	1175.7	1170.4	1165.0	1159.4	1153.6	1147.5	

[a] Standard uncertainties u are $u(\alpha)$ = ±0.005, $u(w)$ = ±2 × 10^{-4} kg, $u(p)$ = ±0.003, $u(T)$ = ±0.012 K, $u(rep)$ = ±0.13 kg·m^{-3}. The combined expanded uncertainty U_c is $U_c(\rho)$ = ±7.80 kg·m^{-3} (level of confidence = 0.95, where k = 2).

**Table 5.** Density correlation parameters for CO_2-loaded aqueous MEA.

Parameters	w_1=0.3	w_1=0.4	w_1=0.5
a_1	0.6802	0.7731	0.7506
a_2	0.001951	0.001354	0.001494
a_3	−2.97 × 10^{-6}	−2.015 × 10^{-6}	−2.237 × 10^{-6}
a_4	2.346	2.164	2.015
AARD (%)	0.15	0.08	0.15
AMD (kg·m^{-3})	4.2	2	3.8
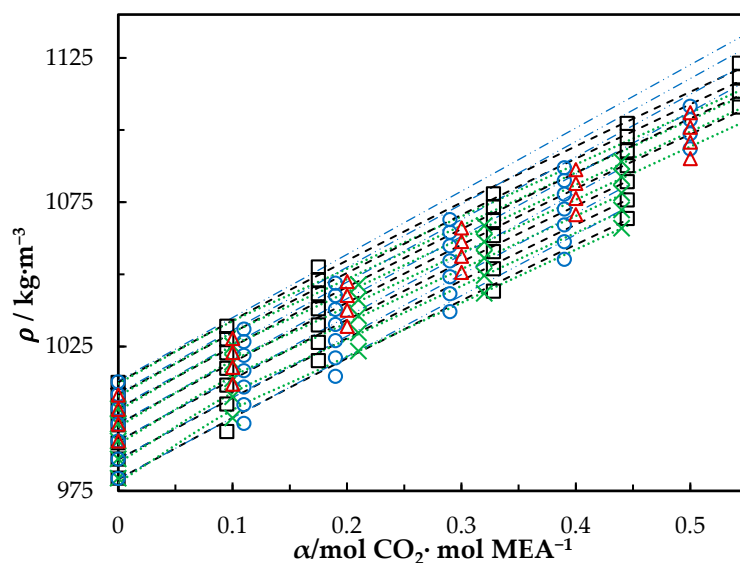
Figure 2. Density of CO_2-loaded MEA ($w_1 = 0.3$) solution at different CO_2 loadings and temperatures (293.15, 303.15, 313.15, 323.15, 333.15, 343.15 and 353.15) K. Data: from this work, '□'; Hartono, Mba and Svendsen [10], 'O'; Han, Jin, Eimer and Melaaen [1], 'x'; Jayarathna, Weerasooriya, Dayarathna, Eimer and Melaaen [8], '△'. Correlation: from this work, '- - -'; Hartono, Mba and Svendsen [10], '-··-'; Han, Jin, Eimer and Melaaen [1], '···'.
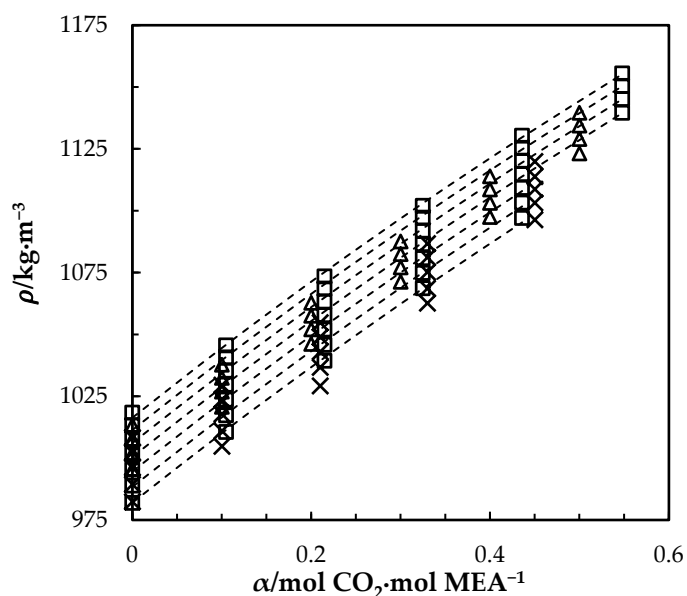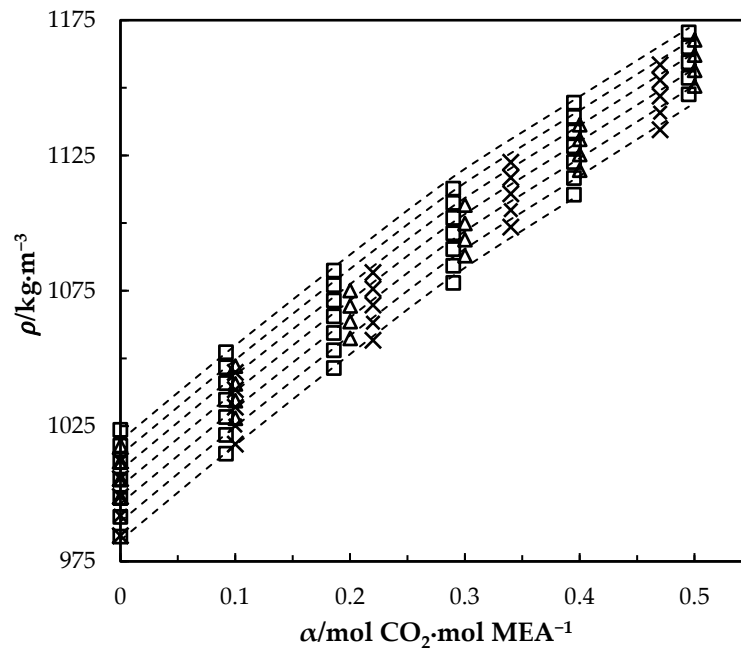

Figure 3. Density of CO_2-loaded MEA ($w_1 = 0.4$) solution at different CO_2 loadings and temperatures (293.15, 303.15, 313.15, 323.15, 333.15, 343.15 and 353.15) K. Data: from this work, '□'; Han, Jin, Eimer and Melaaen [1], 'x'; Jayarathna, Weerasooriya, Dayarathna, Eimer and Melaaen [8], '△'. Correlation: from this work, '- - -'.

Figure 4. Density of CO_2-loaded MEA ($w_1 = 0.5$) solution at different CO_2 loadings and temperatures (293.15, 303.15, 313.15, 323.15, 333.15, 343.15 and 353.15) K. Data: from this work, '□'; Han, Jin, Eimer and Melaaen [1], 'x'; Jayarathna, Weerasooriya, Dayarathna, Eimer and Melaaen [8], '△'. Correlation: from this work, '- - -'.

4.2. Viscosity of MEA (1) + H₂O (2) + CO₂ (3) Mixtures

The Eyring's viscosity model based on absolute rate theory is shown in Equation (5). Here, viscous flow is treated as a chemical reaction considering the elementary process as the motion of a single molecule from one equilibrium position to another over a potential energy barrier [21,22].

$$\eta = \frac{hN_A}{V} exp\left(\frac{\Delta G^*}{RT}\right) \tag{5}$$

where η, V, h, N_A, ΔG^*, R and T are dynamic viscosity, molar volume, Planck's constant, Avogadro's number, free energy of activation for viscous flow, universal gas constant and temperature respectively. For binary liquid mixtures, Equations (5) and (6) were adopted to derive Equation (7) to calculate excess free energy of activation for viscous flow ΔG^{E*}.

$$\frac{\eta}{\eta_{ideal}} = \frac{V_{ideal}}{V} exp\left(\frac{\Delta G^{E*}}{RT}\right) \tag{6}$$

$$\frac{\Delta G^{E*}}{RT} = ln(\eta V) - \sum_{i=1}^{i=2} x_i ln\left(\eta_i V_i^0\right) \tag{7}$$

where x_i, η_i and V_i^0 ($i = 1$ for MEA and $i = 2$ for H₂O) are the mole fraction of components in the mixture, dynamic viscosity and molar volume of pure liquids.

The ΔG^{E*} was evaluated via measured viscosity and density data of aqueous MEA for w_1 from 0.3 to 1 and MEA temperatures from 293.15 K to 363.15 K. Viscosity and density of pure water for this study were taken from Korson, et al. [23] and Kestin, et al. [24]. A Redlich–Kister type correlation was used to fit the derived term $\Delta G^{E*}/RT$ and estimated parameters are given in Table 6. The measured viscosities of aqueous MEA are tabulated with literature data in Table 7. Our previous work has reported viscosities of aqueous MEA from $w_1 = 0.3$ to $w_1 = 0.5$ in Karunarathne, et al. [25]. Figure 5

shows the calculated and fitted ΔG^{E*} and Figure 6 compares the measured with calculated viscosities using the proposed correlation in this work and correlations suggested in the literature.

$$\frac{\Delta G^{E*}}{RT} = x_1 x_2 \sum_{i=0}^{i=2} C_i (1 - 2x_2)^i \tag{8}$$

$$C_i = a_i + b_i(T) \tag{9}$$

Table 6. Parameters of the excess free energy of activation for viscous flow correlation.

| w_1	T/K	Parameters
0–1	298.15–363.15	$a_0 = 16.2$ $b_0 = -0.03473$ $a_1 = -4.853$ $b_1 = 0.008315$ $a_2 = -6.433$
		$b_2 = 0.02065$
	$R^2 = 0.998$	

Table 7. Measured viscosity η of aqueous MEA [a,b,c,d].

w_1	x_1	Measured Viscosity η/mPa·s							
		293.15 K	303.15 K	313.15 K	323.15 K	333.15 K	343.15 K	353.15 K	363.15 K
0.3	0.1122	2.836 2.874 [b] 2.879 [b]	2.109 2.133 [b] 2.130 [b]	1.628 1.628 [b] 1.638 [b] 1.67 [c]	1.290 1.305 [b] 1.318 [b] 1.33 [c]	1.046 1.055 [b] 1.067 [b]	0.866 0.878 [b] 0.874 [b] 0.92 [c]	0.740 0.742 [b] 0.740 [b] 0.77 [c]	0.687
0.4	0.1643	4.285	3.080	2.305 2.28 [c]	1.782 1.75 [c]	1.417	1.154 1.14 [c]	0.960 0.95 [c]	0.808
0.5	0.2278	6.610	4.580 4.69 [d]	3.310 3.39 [c] 3.37 [d]	2.454 2.54 [c] 2.53 [d]	1.915 1.94 [d]	1.528 1.57 [c] 1.54 [d]	1.243 1.28 [c] 1.26 [d]	1.029 1.05 [d]
0.6	0.3067	10.217	6.769 6.92 [d]	4.736 4.77 [d]	3.444 3.45 [d]	2.602 2.62 [d]	2.031 2.04 [d]	1.620 1.62 [d]	1.319 1.34 [d]
0.7	0.4077	15.348	9.823 9.89 [d]	6.664 6.96 [c] 6.69 [d]	4.720 4.94 [c] 4.76 [d]	3.461 3.49 [d]	2.615 2.79 [c] 2.63 [d]	2.029 2.18 [c] 2.04 [d]	1.616 1.63 [d]
0.8	0.5412	20.521	12.840 13.38 [d]	8.534 8.82 [d]	5.937 6.11 [d]	4.295 4.41 [d]	3.217 3.26 [d]	2.483 2.49 [d]	1.962 1.97 [d]
0.9	0.7264	24.027	14.963 15.12 [d]	9.879 10.20 [c] 9.95 [d]	6.829 7.06 [c] 6.88 [d]	4.936 4.94 [d]	3.683 3.81 [c] 3.67 [d]	2.832 2.93 [c] 2.82 [d]	2.222 2.23 [d]
1	1.0000	23.376	14.748 14.77 [d]	10.108 9.61 [c] 9.84 [d]	6.935 6.72 [c] 6.87 [d]	5.067 4.98 [d]	3.834 3.69 [c] 3.72 [d]	2.974 2.85 [c] 2.85 [d]	2.364 2.26 [d]

[a] The pressure was maintained by N_2 gas (p = 4 bar) during the experiments. Standard uncertainties u are $u(w) = \pm 2 \times 10^{-4}$ kg, $u(p) = \pm 0.003$, $u(T) = \pm 0.012$ K, $u(rep) = \pm 0.008$ mPa·s. The combined expanded uncertainty U_c is $U_c(\eta) = \pm 0.016$ mPa·s (level of confidence = 0.95, where k = 2). [b] Hartono, Mba and Svendsen [10], [c] Amundsen, Øi and Eimer [6], [d] Idris, et al. [26].

The viscosities from the correlation were in good agreement with measured data as shown in Figure 6. The proposed correlation was able to calculate viscosities with AARD 1.4% and with AMD 0.79 mPa·s. Table 8 summarizes the AARD and AMD of different suggested correlations.

Figure 5 illustrates the variation of ΔG^{E*} over the whole range of concentrations at different temperatures. At a specific temperature, ΔG^{E*} increases with the increase of MEA concentration until it reaches a maximum at x_{MEA} about 0.41 and then gradually decreases. The ΔG^{E*} decreases with the

increase of temperature while composition for maximum ΔG^{E*} is almost constant. A similar effect was observed for other aqueous amine mixtures [27,28].
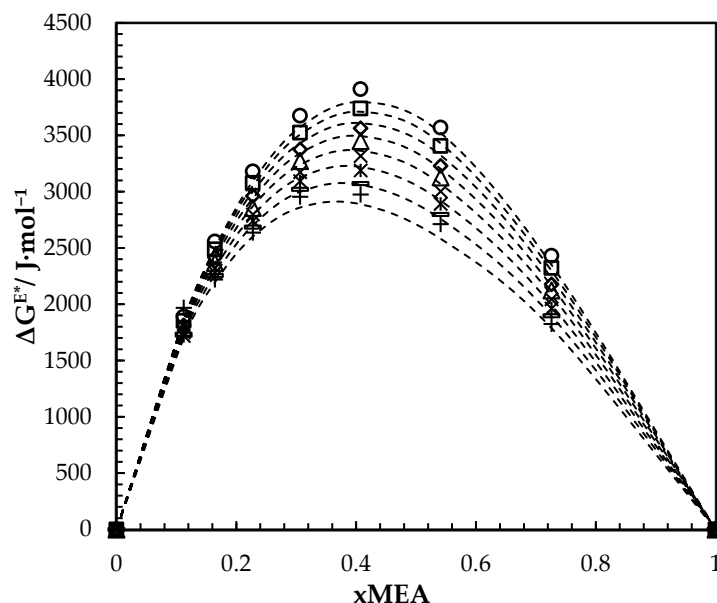
Figure 5. Calculated and fitted ΔG^{E*} for aqueous MEA solutions at different concentrations and temperatures. Calculated: 293.15 K, '○'; 303.15 K, '□'; 313.15 K, '◇'; 323.15 K, '△'; 333.15 K, '×'; 343.15 K, 'ж'; 353.15 K, '-'; 363.15 K, '+'. Correlation: '- - -'.
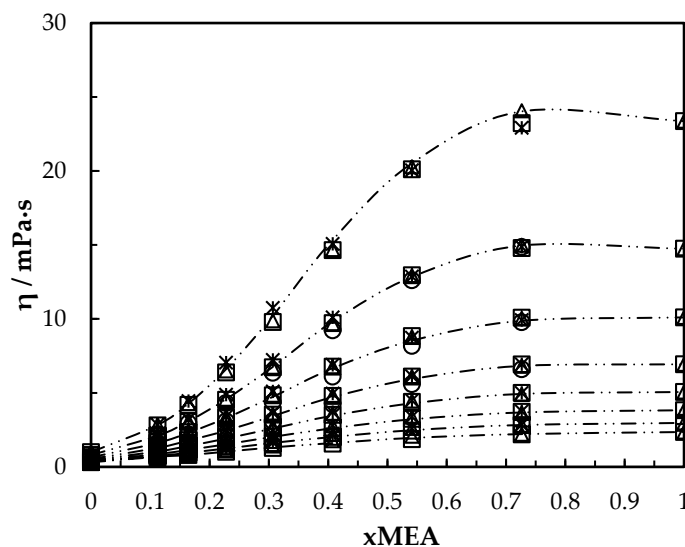
Figure 6. Viscosity of aqueous MEA solutions at different concentrations and temperatures (293.15, 303.15, 313.15, 323.15, 333.15, 343.15, 353.15, 363.15 K). Data: from this work, '-⋯-'. Correlation: from this work, '□'; Hartono, Mba and Svendsen [10], '△'; Arachchige, Aryal, Eimer and Melaaen [11], 'ж'; Islam, Islam and Yeasmin [17], '○'.

Table 8. Average absolute relative deviations and absolute maximum deviation of different suggested correlations for viscosity of aqueous MEA solutions from $w_1 = 0$ to $w_1 = 1$ and 293.15–363.15 K.

Source (s)	No. Parameters	AARD (%)	AMD (mPa·s)
This work	6	1.4	0.79
Hartono, et al. [10]	4	2.4	0.66
Arachchige, et al. [11]	7	3.5	1.1
Islam, et al. [17]	4	5.1	0.59

The excess volume V^E and excess viscosity η^E of aqueous MEA was determined by Equations (10) and (11) to analyze the molecular interaction between MEA and H_2O.

$$V^E = V - (x_1 V_1^0 + x_2 V_2^0) \tag{10}$$

$$\eta^E = \eta - (x_1 \eta_1 + x_2 \eta_2) \tag{11}$$

The $\Delta G^{E*} > 0$ and $V^E < 0$ for the considered MEA concentrations while η^E is negative (< 0) for the water-rich region and gradually become positive (> 0) with the increase of MEA concentration. The $\Delta G^{E*} > 0$ indicates that the viscosity of aqueous MEA solutions has greater viscosities than that of ideal mixtures [29]. The V^E can be negative as a result of the chemical or specific interaction and the structural contribution due to the difference in shape and size [30]. According to Eyring's viscosity model, it can be argued that more energy is required to make necessary holes for molecules to jump in when they are closely packed. The sign of η^E emphasizes strong specific interactions such as hydrogen bonding, which causes complex formations in the amine-rich region and weak interactions in the water-rich region [31].

The viscosity of CO_2-loaded aqueous MEA solutions is given by Table 9 for $w_1 = 0.3$, 0,4 and 0.5 under different CO_2 loading in the temperature range from 293.15–353.15 K. The measured viscosities at $w_1 = 0.3$, $w_1 = 0.4$ and 0.5 are shown in Figures 7–9 respectively with data from the literature. It was observed that the viscosity of solution increases with the increase of CO_2 dissolved in the mixture for all three different MEA concentrations and it decreases with the increase of temperature. The ΔG^* was calculated for both CO_2-loaded and CO_2-unloaded solutions and the difference was considered to develop a correlation as shown in Equations (12) and (13) to predict the viscosity of CO_2-loaded solutions.

Table 9. Measured viscosity of CO_2-loaded (α/mol CO_2 mol·MEA^{-1}) aqueous MEA [a].

x_3	α	Measured Viscosity (η/mPa·s)						
		293.15 K	303.15 K	313.15 K	323.15 K	333.15 K	343.15 K	353.15 K
$w_1 = 0.3$								
0.0000	0.000	2.836	2.109	1.628	1.290	1.046	0.866	0.740
0.0105	0.095	3.103	2.305	1.768	1.397	1.128	0.937	0.788
0.0193	0.175	3.338	2.476	1.910	1.511	1.228	1.021	0.865
0.0355	0.328	3.730	2.764	2.138	1.699	1.384	1.152	0.977
0.0476	0.445	4.164	3.105	2.403	1.913	1.562	1.308	1.118
0.0574	0.543	4.515	3.360	2.602	2.064	1.680	1.403	1.191
$w_1 = 0.4$								
0.0000	0.000	4.285	3.080	2.305	1.782	1.417	1.154	0.960
0.0170	0.105	4.793	3.423	2.567	1.985	1.590	1.302	1.090
0.0341	0.215	5.524	3.944	2.968	2.308	1.851	1.526	1.286
0.0507	0.325	6.496	4.655	3.502	2.726	2.198	1.813	1.524
0.0669	0.436	7.639	5.442	4.084	3.177	2.556	2.111	1.781
0.0826	0.548	8.820	6.203	4.614	3.544	2.821	2.302	1.917
$w_1 = 0.5$								
0.0000	0.000	6.610	4.580	3.310	2.454	1.915	1.528	1.243
0.0205	0.092	7.859	5.378	3.926	2.955	2.303	1.838	1.493
0.0406	0.186	9.518	6.529	4.756	3.594	2.813	2.269	1.866
0.0620	0.290	11.611	7.904	5.710	4.291	3.328	2.667	2.190
0.0825	0.395	14.854	10.073	7.247	5.422	4.227	3.409	2.809
0.1013	0.495	19.348	12.841	9.068	6.678	5.169	4.118	3.365

[a] The pressure was maintained by N_2 gas ($p = 4$ bar) during the experiments. Standard uncertainties u are $u(\alpha) = \pm 0.005$, $u(w) = \pm 2 \times 10^{-4}$ kg, $u(p) = \pm 0.003$, $u(T) = \pm 0.012$ K, $u(rep) = \pm 0.008$ mPa·s.
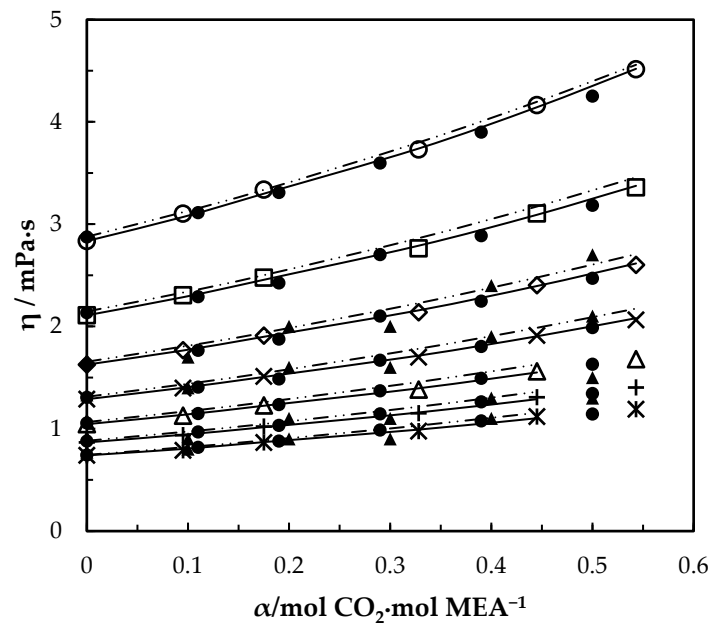
Figure 7. Viscosity of CO_2-loaded aqueous MEA ($w_1 = 0.3$) solutions at different CO_2 loadings and temperatures. Data: from this work, 293.15 K, '○'; 303.15 K, '□'; 313.15 K, '◇'; 323.15 K, '×'; 333.15 K, '△'; 343.14 K, '+'; 353.15 K, 'ж'; Hartono, Mba and Svendsen [10], '●'; Amundsen, Øi and Eimer [6], '▲'. Correlation: from this work, '- - -'; Hartono, Mba and Svendsen [10], '-···-'.
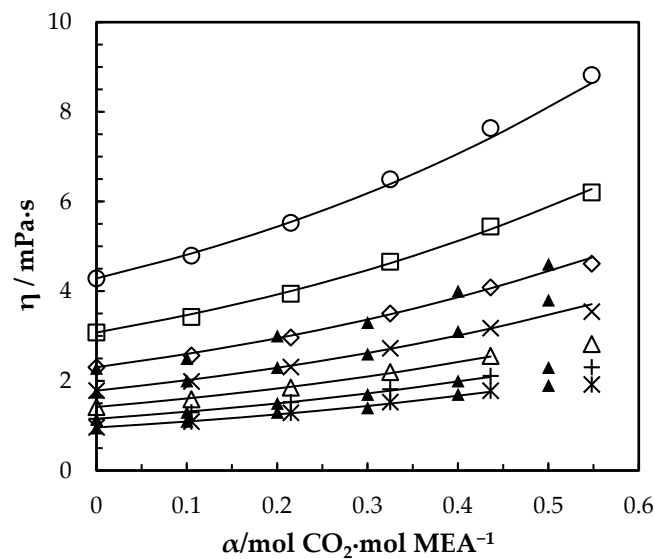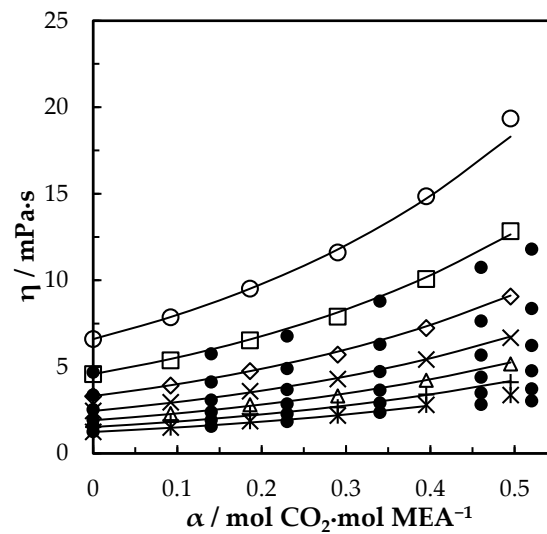

Figure 8. Viscosity of CO_2-loaded aqueous MEA ($w_1 = 0.4$) solutions at different CO_2 loadings and temperatures. Data: from this work, 293.15 K, '○'; 303.15 K, '□'; 313.15 K, '◇'; 323.15 K, '×'; 333.15 K, '△'; 343.14 K, '+'; 353.15 K, 'ж'; Amundsen, Øi and Eimer [6], '▲'. Correlation: from this work, '—'.

The combined expanded uncertainty U_c is $U_c(\eta) = \pm 0.036$ mPa·s (level of confidence = 0.95, where $k = 2$).

$$ln(V\eta)_{CO2\ loaded} = ln(V\eta)_{unloaded} + f(x_3, T) \tag{12}$$

$$f(x_3, T) = x_3(d_1 + d_2 T + d_3 x_3) \tag{13}$$

Figure 9. Viscosity of CO_2-loaded aqueous MEA ($w_1 = 0.5$) solutions at different CO_2 loadings and temperatures 293.15 K, '○'; 303.15 K, '□'; 313.15 K, '◇'; 323.15 K, 'x'; 333.15 K, '△'; 343.14 K, '+'; 353.15 K, 'ж'; Idris, Kummamuru and Eimer [26], '●'. Correlation: from this work, '—'.

The calculated AARD shows that the predicted and measured viscosities are in good agreement and parameters for the correlation are given in Table 10. The molar volume of CO_2-loaded aqueous MEA solutions was calculated using the mole fraction of dissolved CO_2 that was determined via CO_2 loading analysis. In a real solution, CO_2 reacts with MEA to form carbamate and bicarbonate ions and the solution becomes an electrolyte. Here it is assumed as unreacted and molar volumes were calculated using Equation (14) [32]. This approach was taken to represent dissolved CO_2 in aqueous MEA [7,10,26] and used in the viscosity correlation by Hartono, Mba and Svendsen [10].

$$V_{loaded} = \frac{\sum_1^3 x_i M_i}{\rho_{loaded}}$$
(14)

Table 10. Parameters of viscosity correlation for CO_2-loaded solutions.

T/K	Parameters	$w_1 = 0.3$	$w_1 = 0.4$	$w_1 = 0.5$
298.15–343.15	d_1	4.536	2.554	8.533
	d_2	0.006765	0.01205	−0.0037
	d_3	12.08	19.46	17.79
AARD (%)		0.58	1.13	1.25
AMD (mPa·s)		0.03	0.22	1.04

The variations of ΔG^* with CO_2 loading and temperature are shown in Figure 10a–c. For CO_2 loaded solutions, ΔG^* increases with the increase of dissolved CO_2 while it decreases with temperature. The amount of ions present in the solution due to the formation of carbamate and bicarbonate increases with the CO_2 loading, which results in higher ionic strength as discussed by Matin, et al. [33]. At higher ionic strengths, ions can create an ionic field that attract water molecules to form clusters, which leads to higher viscosity. The increase of ΔG^* implies the increase of potential barrier for the molecule transfer. The molecular interactions among the molecules in CO_2-loaded solutions may enhance the strength of energy barrier more than that of unloaded solutions. The correlation given in Equation (15) was proposed to fit ΔG^* for the CO_2-loaded aqueous MEA of $w_1 = 0.3$, 0,4 and 0.5. On the other hand, since the Eyring's viscosity model is based on the motion of individual molecules from one equilibrium position to another; it does not explain the effect of hydrogen bond network on the bulk viscosity of the various CO_2-loaded aqueous [34] MEA solutions. Further, the model has molar volume as a parameter

that needs to be known to calculate the viscosity. This can be done by using calculated molar volume from density data measured under the same conditions or from a correlation.

$$\Delta G^*_{CO2\ loaded} = \Delta G^*_{unloaded} + x_3 RT(d_1 + d_2 T + d_3 x_3) \tag{15}$$
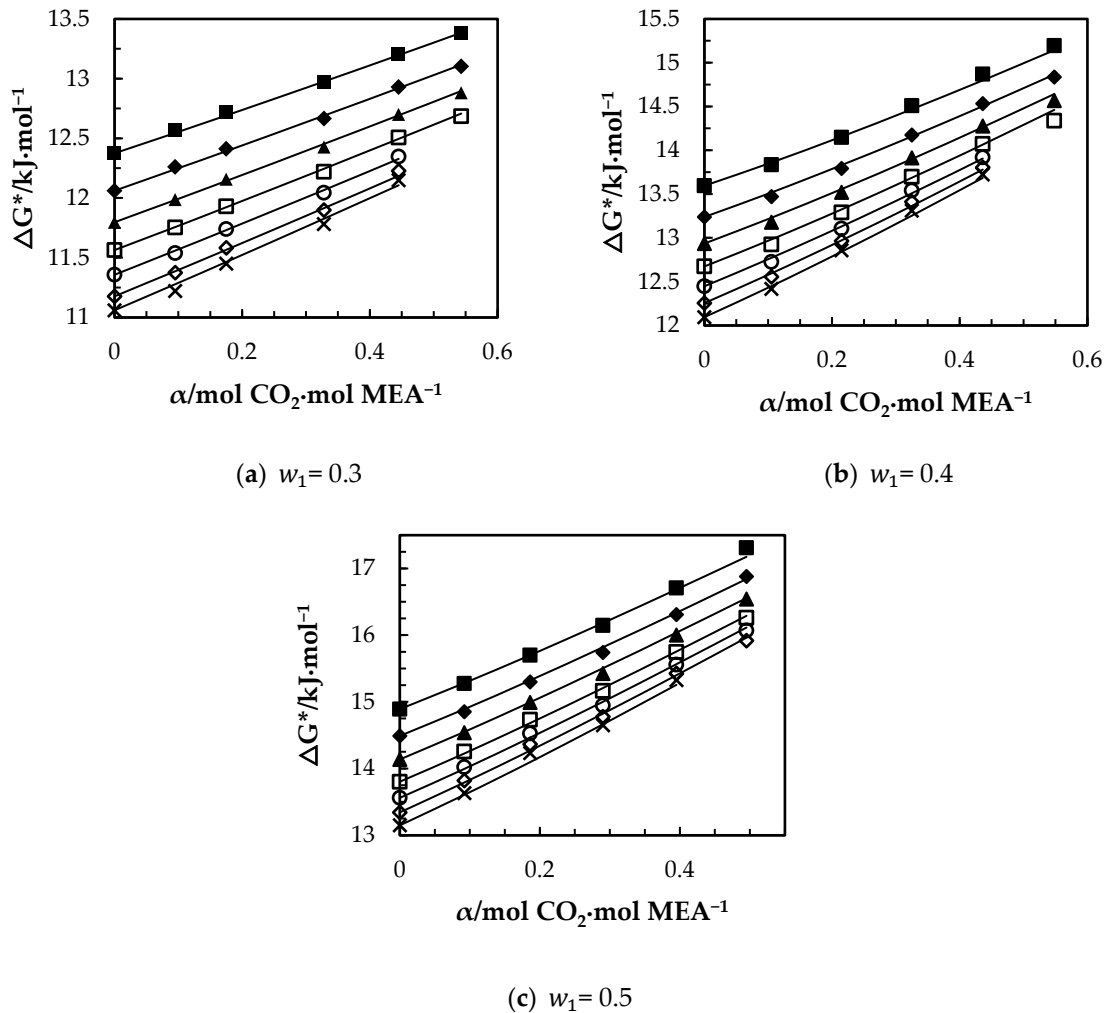
(**a**) $w_1 = 0.3$

(**b**) $w_1 = 0.4$

(**c**) $w_1 = 0.5$

Figure 10. Variation of free energy of activation for viscous flow of CO_2-loaded aqueous MEA: (**a**) $w_1 = 0.3$, (**b**) $w_1 = 0.4$, (**c**) $w_1 = 0.5$ solutions at different CO_2 loadings and temperatures of $T = 293.15$ K, '■'; 303.15 K, '♦'; 313.15 K, '▲'; 323.15 K, '□'; 333.15 K, '○'; 343.15 K, '◇'; 353.15 K, 'x' from Eyring's viscosity model. '—' from correlation in Equation (15).

The relationship between $Rln(\eta V/(hN_A))$ vs. $1/T$ gives information about activation parameters in which enthalpy of activation for viscous flow ΔH^* is given by the gradient and entropy of activation for viscous flow ΔS^* is given by the intercept of the curve under different mole fractions of the components. The ΔG^*, ΔH^* and ΔS^* are connected through the equation $\Delta G^* = \Delta H^* - T\Delta S^*$. Accordingly, Eyring's viscosity model is given as follows.

$$\eta = \frac{hN_A}{V} exp\left(\frac{\Delta H^*}{RT} - \frac{\Delta S^*}{R}\right) \tag{16}$$

Tables 11 and 12 list the calculated ΔG^* directly from Eyring's viscosity model, and ΔH^* and ΔS^* from the relation shown in Equation (16). It is observed that ΔG^*, ΔH^* and ΔS^* are positive for all considered mixtures while ΔH^* is greater than $T\Delta S^*$. This reveals that the influence of enthalpy of activation to the free energy of activation is greater than entropy of activation for viscous flow. Further,

this work shows how ΔG^* can be regarded as a parameter to regress and also can be regarded as a parameter with a physical meaning.

Table 11. Free energy of activation for viscous flow $\Delta G^*/\text{kJ·mol}^{-1}$ for CO_2-loaded aqueous MEA.

	T/K	293.15	303.15	313.15	323.15	333.15	343.15	353.15
w_1	x_3				Free Energy $\Delta G^*/\text{kJ·mol}^{-1}$			
	0.0000	12.375	12.062	11.798	11.564	11.358	11.177	11.060
	0.0105	12.571	12.262	11.988	11.753	11.539	11.376	11.222
0.3	0.0193	12.721	12.413	12.159	11.931	11.740	11.583	11.451
	0.0355	12.970	12.667	12.428	12.220	12.044	11.900	11.783
	0.0476	13.210	12.931	12.702	12.507	12.347	12.228	12.150
	0.0574	13.382	13.105	12.883	12.685			
	0.0000	13.595	13.240	12.936	12.674	12.448	12.255	12.094
	0.0170	13.835	13.471	13.179	12.924	12.726	12.556	12.419
0.4	0.0341	14.148	13.793	13.521	13.291	13.105	12.965	12.860
	0.0507	14.509	14.175	13.914	13.698	13.540	13.413	13.312
	0.0669	14.870	14.534	14.278	14.072	13.919	13.807	13.725
	0.0826	15.194	14.837	14.568	14.337			
	0.0000	14.891	14.489	14.137	13.802	13.560	13.344	13.148
	0.0205	15.275	14.853	14.538	14.255	14.022	13.819	13.631
0.5	0.0406	15.701	15.299	14.992	14.733	14.526	14.366	14.230
	0.0620	16.147	15.741	15.426	15.165	14.945	14.779	14.648
	0.0825	16.707	16.309	16.002	15.747	15.559	15.427	15.325
	0.1013	17.311	16.879	16.543	16.262	16.069	15.918	

Table 12. Free energy of activation for viscous flow $\Delta G^*/\text{kJ·mol}^{-1}$ for CO_2-loaded aqueous MEA.

w_1	x_3	$\Delta H^*/\text{kJ·mol}^{-1}$	$\Delta S^*/\text{J·(mol·K)}^{-1}$
	0.0000	18.834	22.301
	0.0105	19.150	22.696
0.3	0.0193	18.902	21.360
	0.0355	18.716	19.895
	0.0476	18.400	18.003
	0.0574	20.173	23.234
	0.0000	20.897	25.215
	0.0170	20.688	23.742
0.4	0.0341	20.377	21.642
	0.0507	20.266	20.026
	0.0669	20.379	19.209
	0.0826	23.540	28.578
	0.0000	23391	29.339
	0.0205	23147	27.247
0.5	0.0406	22773	24.566
	0.0620	23389	25.142
	0.0825	23381	23.248
	0.1013	25441	28.114

5. Conclusions

Densities and viscosities of MEA (1) + H_2O (2) mixtures have been measured for the mass fraction w_1 from 0.3 to 1 and temperatures in the range 273.15 K to 363.15 K. The density data were correlated using the correlation proposed by Aronu, Hartono and Svendsen for w_1 from 0.3 to 0.9. The accuracy of the measured density with correlation predictions are acceptable as the AARD is 0.12% and AMD is 3.45 kg·m^{-3}. The viscosity data were correlated using a Redlich–Kister type polynomial fitted to the excess free energy of activation for viscous flow ΔG^{E*} obtained via the Eyring's viscosity model for

the w_1 from 0 to 1 and temperatures in a range from 273.15 K to 363.15 K. The developed correlation was able to represent the measured viscosities with AARD = 1.4% and AMD = 0.79 mPa·s, which is acceptable in engineering calculations.

The densities of CO_2-loaded aqueous MEA solutions were measured at temperatures ranging from 293.15 K to 353.15 K for w_1 of 0.3, 0.4 and 0.5. Density of CO_2-loaded solutions increases with the CO_2 loading and decreases with temperature. The density correlation proposed by Aronu, Hartono and Svendsen was modified to correlate the density data. The AMD between correlated and experimental densities are 4.2 kg·m^{-3}, 2 kg·m^{-3} and 4.5 kg·m^{-3} for CO_2-loaded solutions with w_1 of 0.3, 0.4 and 0.5 respectively.

The viscosities of CO_2-loaded aqueous MEA solutions were measured at temperatures ranging from 293.15 K to 353.15 K for w_1 of 0.3, 0.4 and 0.5. As CO_2 loading increased, the viscosity increased and the viscosity decreased with the increase of temperature. A correlation was proposed for the free energy of activation for viscous flow using CO_2 mole fraction and temperature to correlate viscosity data. The AMD between correlated and experimental viscosities are 0.03 mPa·s, 0.22 mPa·s and 1.04 mPa·s for CO_2-loaded solutions with w_1 of 0.3, 0.4 and 0.5 respectively. The proposed correlation is recommended to use in engineering calculations.

References

1. Han, J.; Jin, J.; Eimer, D.A.; Melaaen, M.C. Density of water (1) + Monoethanolamine (2) + CO2 (3) from (298.15 to 413.15) K and surface tension of water (1) + Monoethanolamine (2) from (303.15 to 333.15) K. *J. Chem. Eng. Data* **2012**, *57*, 1095–1103. [CrossRef]

2. Nwaoha, C.; Saiwan, C.; Supap, T.; Idem, R.; Tontiwachwuthikul, P.; Rongwong, W.; Al-Marri, M.J.; Benamor, A. Carbon dioxide (CO2) capture performance of aqueoustri-solvent blends containing 2-amino-2-methyl-1-propanol (AMP) and methyldiethanolamine (MDEA) promoted by diethylenetriamine (DETA). *Int. J. Greenh. Gas Control* **2016**, *53*, 292–304. [CrossRef]

3. Kidnay, A.J.; Parrish, W.R. *Fundamentals of Natural Gas Processing*; Taylor & Francis Group: Boca Raton, FL, USA, 2006.

4. Maham, Y.; Teng, T.T.; Hepler, L.G.; Mather, A.E. Densities, excess molar volumes, and partial molar volumes for binary mixtures of Water with Monoethanolamine, Diethnolamine, and Triethanolamine from 25 to 80 °C. *J. Solut. Chem.* **1994**, *23*, 195–205. [CrossRef]

5. Yang, F.; Wang, X.; Wang, W.; Liu, Z. Densities and excess properties of primary amines in alcoholic solutions. *J. Chem. Eng. Data* **2013**, *58*, 785–791. [CrossRef]

6. Amundsen, T.G.; Øi, L.E.; Eimer, D.A. Density and viscosity of monoethanolamine + water + carbon dioxide from (25 to 80) °C. *J. Chem. Eng. Data* **2009**, *54*, 3096–3100. [CrossRef]

7. Jayarathna, S.A.; Jayarathna, C.K.; Kottage, D.A.; Dayarathna, S.; Eimer, D.A.; Melaaen, M.C. Density and surface tension measurement of partially carbonated aqueous monoethanolamine solutions. *J. Chem. Eng. Data* **2013**, *58*, 343–348. [CrossRef]

8. Jayarathna, S.; Weerasooriya, A.; Dayarathna, S.; Eimer, D.A.; Melaaen, M.C. Densities and surface tensions of CO2 loaded aqueous monoethanolamine solution with r = (0.2 to 0.7) at T = (303.15 to 333.15) K. *J. Chem. Eng. Data* **2013**, *58*, 986–992. [CrossRef]

9. Weiland, R.H.; Dingman, J.C.; Cronin, D.B.; Browning, G.J. Density and viscosity of some partially carbonated aqueous alkanolamine solutions and their blends. *J. Chem. Eng. Data* **1998**, *43*, 378–382. [CrossRef]

10. Hartono, A.; Mba, E.O.; Svendsen, H.F. Physical properties of partially CO2 loaded aqueous monoethanolamine (MEA). *J. Chem. Eng. Data* **2014**, *59*, 1808–1816. [CrossRef]

11. Arachchige, U.S.P.R.; Aryal, N.; Eimer, D.A.; Melaaen, M.C. Viscosities of pure and aqueous solutions of Monoethanolamine (MEA), Diethanolamine (DEA), and N-Methyldiethanolamine (MDEA). In Proceedings of the Annual Transactions of the Nordic Rheology Society, Copenhagen, Demark, 12–14 June 2013.

12. Hsu, C.-H.; Li, M.-H. Viscosities of Aqueous Blended Amines. *J. Chem. Eng. Data* **1997**, *42*, 714–720. [CrossRef]

13. Versteeg, G.F.; Van Swaaij, W.P.M. Solubility and diffusivity of acid gases (carbon dioxide, nitrous oxide) in aqueous alkanolamine solutions. *J. Chem. Eng. Data* **1988**, *33*, 29–34. [CrossRef]

14. Aronu, U.E.; Hartono, A.; Svendsen, H.F. Density, viscosity, and N2O solubility of aqueous amino acid salt and amine amino acid salt solutions. *J. Chem. Thermodyn.* **2012**, *45*, 90–99. [CrossRef]

15. McAllister, R.A. The viscosity of liquid mixtures. *AIChE. J.* **1960**, *6*, 427–431. [CrossRef]

16. Redlich, O.; Kister, A.T. Algebraic representation of thermodynamic properties and the classification of solutions. *Ind. Eng. Chem.* **1948**, *40*, 345–348. [CrossRef]

17. Islam, M.N.; Islam, M.M.; Yeasmin, M.N. Viscosity of aqueous solution of 2-methoxyethanol, 2-ethoxyethanol, and ethanolamine. *J. Chem. Thermodyn.* **2004**, *36*, 889–893. [CrossRef]

18. Eyring, H. Viscosity, Plasticity, and Diffusion as example of absolute reaction rates. *J. Chem. Phys.* **1936**, *4*, 283–291. [CrossRef]

19. JCGM. Evaluation of measurement data—Supplement 1 to the Guide to the Expression of Uncertainty In Measurement—Propagation of Distributions Using a Monte Carlo Method. In *JCGM 101: 2008*; JCGM: Sevres, France, 2008.

20. Ellison, S.L.R.; Williams, A. *Eurachem/CITAC Guide: Quantifying Uncertainty in Analytical Measurement*, 3rd ed.; 2012; Available online: http://www.eurachem.org (accessed on 15 November 2019).

21. Nhaesi, A.H. A Study of the Predictive Models for the Viscosity of Multi-Component Liquid Regular Solutions. Ph.D. Thesis, University of Windsor, Windsor, UK, 1998. Available online: https://core.ac.uk/download/pdf/72774384.pdf (accessed on 15 November 2019).

22. Macías-Salinas, R.; Aquino-Olivos, M.A.; García-Sánchez, F. Viscosity modelling of reservoir fluids over wide temperature and pressure ranges. *Chem. Eng. Trans.* **2013**, *32*, 1573–1578. [CrossRef]

23. Korson, L.; Hansen, W.D.; Millero, F.J. Viscosity of water at various temperatures. *J. Phys. Chem.* **1969**, *73*, 34–39. [CrossRef]

24. Kestin, J.; Sokolov, M.; Wakeham, W.A. Viscosity of liquid water in the range −8 °C to 150 °C. *J. Phys. Chem. Ref. Data* **1978**, *7*, 941–948. [CrossRef]

25. Karunarathne, S.S.; Eimer, D.A.; Øi, L.E. Evaluation of systematic error and uncertainty of viscosity measurements of mixtures of monoethanol amine and water in coaxial cylinder rheometers. *Int. J. Model. Optim.* **2018**, *8*, 260–265. [CrossRef]

26. Idris, Z.; Kummamuru, N.B.; Eimer, D.A. Viscosity measurement of unloaded and CO2-loaded aqueous monoethanolamine at higher concentrations. *J. Mol. Liq.* **2017**, *243*, 638–645. [CrossRef]

27. Hartono, A.; Svendsen, H.F. Density, viscosity, and excess properties of aqueous solution of diethylenetriamine (DETA). *J. Chem. Thermodyn.* **2009**, *41*, 973–979. [CrossRef]

28. Maham, Y.; Liew, C.N.; Mather, A.E. Viscosities and Excess Properties of Aqueous Solutions of Ethanolamines from 25 to 80 °C. *J. Solut. Chem.* **2002**, *31*, 743–756. [CrossRef]

29. Heric, E.L.; Brewer, J.G. Viscosity of some binary liquid nonelectrolyte mixtures. *J. Chem. Eng. Data* **1967**, *12*, 574–583. [CrossRef]

30. Mahajan, A.R.; Mirgane, S.R. Excess molar volumes and viscosities for the binary mixtures of n-Octane, n-Decane, n-Dodecane, and n-Tetradecane with Octan-2-ol at 298.15 K. *J. Thermodyn.* **2013**, *2013*, 1–11. [CrossRef]

31. Idris, Z.; Kummamuru, N.B.; Eimer, D.A. Viscosity measurement and correlation of unloaded and CO2 loaded 3-Amino-1-propanol solution. *J. Chem. Eng. Data* **2018**, *63*, 1454–1459. [CrossRef]

32. Stec, M.; Spietz, T.; Wieclaw-Solny, L.; Tatarczuk, A.; Wilk, A.; Sobolewski, A. Density of unloaded and CO2-loaded aqueous solutions of piperazine and 2-amino-2-methyl-1-propanol and their mixtures from 293.15 to 333.15 K. *Phys. Chem. Liq.* **2015**, *54*, 475–486. [CrossRef]

33. Matin, N.S.; Remias, J.E.; Liu, K. Application of electrolyte-NRTL model for prediction of the viscosity of carbon dioxide loaded aqueous amine solutions Ind. *Eng. Chem. Res* **2013**, *52*, 16979–16984. [CrossRef]

34. Perticaroli, S.; Mostofian, B.; Ehlers, G.; Neuefeind, J.C.; Diallo, S.O.; Stanley, C.B.; Daemen, L.; Egami, T.; Katsaras, J.; Cheng, X.; et al. Structural relaxation, viscosity, and network connectivity in a hydrogen bonding liquid. *Phys. Chem. Chem. Phys.* **2017**, *19*, 25859–25869. [CrossRef]